Surface of amorphous semiconductors and their contacts with metals*

Horng-Yhi Wey†‡
Department of Physics, The University of Chicago, Chicago, Illinois 60637
(Received 25 August 1975)

Contacts formed by rf sputtering of a chalcogenide glass onto several metals, including Ag, Al, Au, Cu, Mo, Ni, Pd, Pt, Sb, Ta, Te, and nichrome were studied by measuring photoconductivity, contact photovoltage, parallel capacitance $C_p(\omega)$ and resistance $R_p(\omega)$, and the I-V characteristic. Aging and annealing effects on the contact properties were found with several metals. In the case of some contact metals alloying produced high- or low-resistance regions depending on preparation conditions. Adsorption of H_2O and other polar molecules was found to shift the surface potential and thus the surface photovoltage. Evidence of the presence of a space-charge region and for compound formation (or alloying) are discussed. The width of the space-charge region was found to be between 300 and 500 Å. This corresponds to a density of localized gap states between 2×10^{17} $eV^{-1}cm^{-3}$ to 8×10^{17} $eV^{-1}cm^{-3}$ near the Fermi level. The small size of the field effect in these materials implies a density of interface states of about 10^{14} $eV^{-1}cm^{-2}$. No rectification was observed up to fields of 5×10^{4} V/cm. This may be understood in terms of ambipolar conduction in the space-charge region of the nearly intrinsic amorphous semiconductor.

I. INTRODUCTION

Surprisingly little attention has been paid to the properities of surfaces and contacts of amorphous semiconductors although the behavior of contacts appears to be important for understanding the switching phenomena in these materials.[1-3] This lack of attention is particularly interesting in view of the fact that in the field of crystalline semiconductors, the rectifying and injection properties of contacts[4] led to the invention of a variety of important devices.[5] Contacts to amorphous semiconductors[6,7] indeed do not reveal striking effects: they show no polarity dependence and their resistance is usually negligible compared to that of the bulk material. Nevertheless we believe the properties of contacts are important for many conduction processes, particularly for those at high fields.[1,8,9] Furthermore, since most of the measurements on amorphous semiconductors are carried out on thin films, it is essential to know the properties of the surface and interfacial regions in order to deduce from thin-film measurements the properties of the bulk material. In this paper, we present studies of several effects associated with contacts and the surface of an amorphous semiconductor.

For crystalline semiconductor contacts, a number of techniques[5] have been employed to obtain information about the barrier height, surface states, and the screening length; for instance, I-V characteristic, frequency and bias dependence of the capacitance $C(\omega)$ and $C(V)$, internal photoemission, and the contact and surface photovoltage. In the case of crystalline semiconductors it is rather easy to determine the space-charge capacitance and thus the screening length from $C(V)$ and $C(\omega)$ measurements because the Fermi level lies near the conduction-band or valence-band edge; thus the resistivity of the bulk region is much less than that of the contact region, and the voltage drop is confined mainly to the contact region. In amorphous semiconductors, on the other hand, the Fermi level usually lies close to the gap center.[10] The resistivity of the contact region is thus comparable with or even less than that of the bulk region. The applied voltage drop is therefore mainly across the bulk region. We therefore found it difficult to extract information about the contact region from the frequency and bias dependence of total capacitance. These measurements yield, however, information about the presence of high-resistance alloy regions near the contacts. The space-charge width was obtained from the wavelength dependence of the photovoltage.

II. SAMPLE PREPARATION AND EXPERIMENTAL TECHNIQUE

A. Sample preparation

The geometry of the samples is shown in Fig. 1. Semitransparent metal electrodes, about 200 Å thick, were evaporated or dc sputtered onto a Corning 7059 glass substrate. A chalcogenide glass film of composition $Ge_{16}As_{35}Te_{28}S_{21}$ about 1–10 μm thick was then rf sputtered. We then evaporated or dc sputtered another metal electrode on top of the chalcogenide semiconductor film as the common electrode. The cross-sectional area of each sample was about 0.20 cm^2. The sputtering target was hot-pressed under an inert gas cover from a vacuum-melted constituent of 99.999% purity.[11] The target was mounted in a Mathis SP-310 rf diode sputtering system atop a

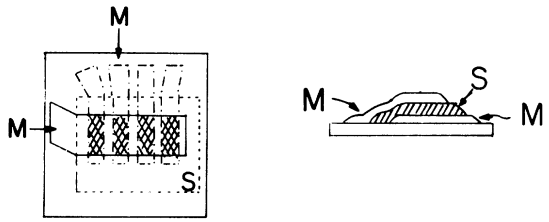

FIG. 1. Structure of samples. A common semitransparent metal electrode was evaporated on the substrates, followed by radio frequency sputtering on amorphous chalcogenide film S. Four thin electrodes of different metals were then evaporated one after the other onto S and the substrate without breaking the vacuum.

turbo pump instead of a conventional diffusion pump to prevent possible oil vapor contamination of the samples. Before admitting the argon sputtering gas the background pressure was about 3×10^{-6} Torr. Target and substrate stages were water cooled. Normal sputtering pressure was 3.5 mTorr of ultrapure argon. The average dc component of the applied rf voltage was 500 V. A sputtering rate of about 55 Å/min was maintained fairly constant for all samples. Substrates were kept electrically floating so that samples of nearly the same composition as the target material were obtained within the accuracy of electron microprobe analysis.[12,13] Substrates were illuminated by ultraviolet light for a short time before closing the sputtering system to eliminate the accumulation of static charges which appeared to act as nucleation centers during rf sputtering.

B. Experimental technique and apparatus

The resistance of each sample was measured and recorded immediately after the sample was made before placing it into a dessicator to await further studies. The resistance of each sample was checked periodically. Most samples showed stable resistances except for some samples with Cu, Ag electrodes, whose resistance increased with time. Strong chemical reactions seem to occur at the Ag and Cu contacts. These manifested themselves in the appearance of a steady open circuit dc voltage between opposite electrodes. The thin metal electrodes gradually disappeared by reacting with the semiconductor.

The I-V characteristic, contact photovoltage, and the equivalent parallel capacitance C_p and resistance R_p were then measured for each sample. Because of the high resistivity of the amorphous semiconductor ($\sim10^8$ Ω cm at 300 K, conductivity activation energy $\Delta E\sim0.57$ eV), a highly insulated and well shielded cryostat was used. Furthermore, in measuring the contact photovoltage, it was found necessary to eliminate the thermovoltage due to the temperature difference between the two counter electrodes. A specially designed cryostat which has the sample immersed in a thermal exchange He gas as shown in Fig. 2, provides high insulation, good thermal stabilization, and capability for measuring the contact and surface photovoltages.

As shown in Fig. 2, the cryostat consists of four chambers (labeled A, B, C, and D). A diffusion pump assembly was connected to the outermost chamber A for vacuum thermal insulation. The sample chamber B is filled with 1-atm He gas so that the two counterelectrodes of a sandwich-type sample remain at nearly equal temperature. The temperature in the sample chamber B can be controlled by the heater and by changing the He heat exchange gas pressure in heat conduction chamber C. Chamber D is the heat sink chamber filled with liquid nitrogen or a mixture of dry ice and alcohol. Temperature stabilization to within 0.05 deg can be achieved for a long time. When studying the effect of ambient gases on the surface photovoltage, a thin tube was connected from the gas inlet to the bottom of the cryostat to provide a steady gas flow.

Monochromatic light from a tungsten halogen lamp through a Perkin-Elmer monochromater was focused on the top electrode of the sample. A high input impedance ($\sim10^{14}$ Ω) Keithley 610 C electrometer was used to measure the open circuit

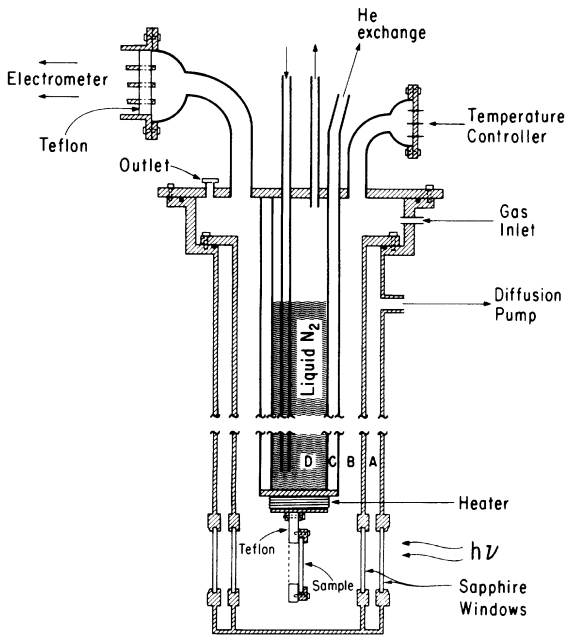

FIG. 2. Variable temperature optical cryostat used for contact photovoltage and surface photovoltage measurements. The sample is immersed in helium exchange gas to minimize the temperature difference between the front and back electrodes.

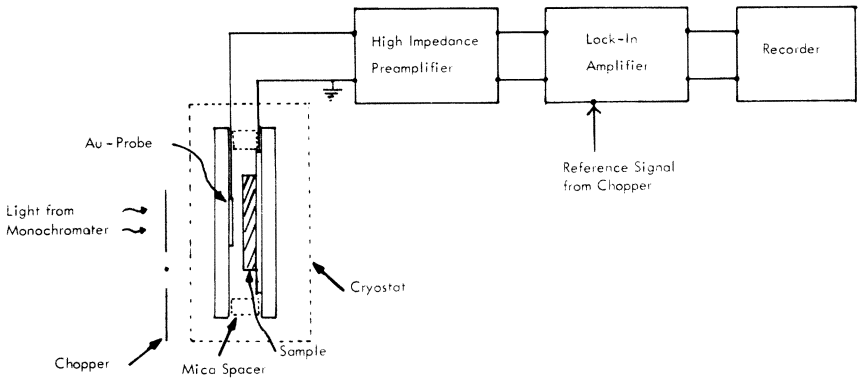

FIG. 3. Schematic diagram of apparatus used for measuring surface photovoltage.

dc photovoltage across the electrodes when the sample was illuminated. The photovoltage was measured as a function of photon energy, light intensity, and temperature.

The surface photovoltage was measured as shown in the schematic diagram of Fig. 3. The amorphous semiconductor film about 5 μm was sputtered on top of a molybdenum electrode which was dc sputtered first on the substrate glass. The capacitive probe electrode of semitransparent gold film evaporated on a substrate glass was then mounted on top of the sample but separated from it by a mica spacer about 30 μm thick. Chopped light was directed through the gold film onto the semiconductor surface. The change of the surface potential was detected by the gold-film probe and amplified with a high input impedance amplifier and a PAR lock-in amplifier.

The parallel capacitance and resistance of the sandwich samples were measured as a function of frequency and temperature, using a specially constructed bridge.[14] Because the amorphous semiconductors studied were of a very lossy material (high dissipation factor), no commercial impedance bridge was operative at low frequencies. An impedance bridge was constructed by modifying the ordinary Wheatstone Bridge such that the parallel capacitance and resistance could be measured simultaneously at very low frequencies. Stray capacitances were minimized by circuit construction and taken into consideration in the computer program used for calculating the sample impedance from the measured data.

III. EXPERIMENTAL RESULTS

A. Contact photovoltage

Figure 4 shows the photovoltage at room temperature as a function of photon energies covering the range from 0.6 eV, where the sample is transparent, through the onset of absorption at 1.2 eV into the visible spectral range, where the sample is highly absorbent. The photon energies at which the product of the absorption coefficient α and the sample thickness d is equal to 1 and 5, respectively, are indicated by arrows on the top scale of the figures. At photon energies $h\nu < 1.7$ eV, the photons reach both the top and the bottom electrodes. At higher photon energies $h\nu > 1.7$ eV the sample is optically dense and therefore only the region adjacent to the top electrode is illuminated. As a consequence, the photovoltage is the sum of the photovoltages generated at both contacts for $h\nu < 1.7$ eV and equal to the photovoltage of the

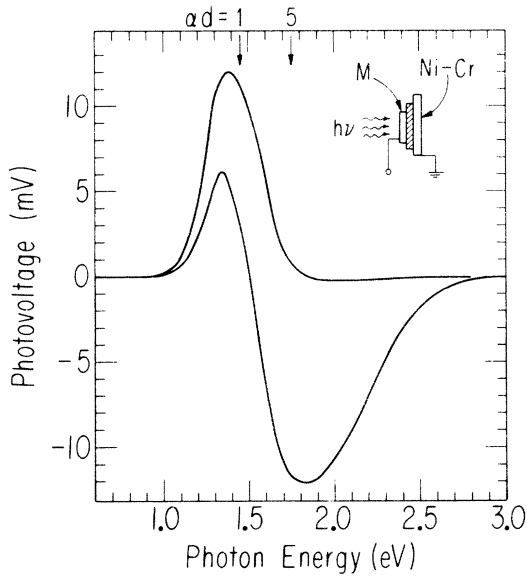

FIG. 4. Spectral response of the photovoltage of two samples, one with top electrode M = Sb, the other with M = Ni-Cr. The photovoltage is not normalized. The photon flux at 1.4, 2, and 3 eV was 10^{14}, 10^{13}, and 10^{12} $cm^{-2}\,sec^{-1}$, respectively. Arrows on top scale show the product of absorption coefficient α and sample thickness d. For $h\nu > 1.7$ eV the photons are absorbed before reaching the back electrode. The photovoltage (zero for M = Sb) is thus solely generated near the top electrode in this high-energy range.

top electrode only, at $h\nu > 1.7$ eV. The absence of any photovoltage at large photon energies in Fig. 4 indicates that the photovoltage of the Sb contact is close to zero. The large peak centered at $h\nu \sim 1.4$ eV in Fig. 4 is therefore caused by the photovoltage generated at the Ni-Cr contact. If there exists a space charge region near the Ni-Cr contact, the so-called contact photovoltage (or barrier photovoltage) will be generated when this region is illuminated. Electron-hole pairs produced by the absorption of photons will be separated before recombination due to the strong internal field in the space charge region. The positive sign of the photovoltage indicates that the space-charge region adjacent to the Ni-Cr contact is negative, which means that the internal field at the surface points into the semiconductor.

Figure 4 shows also the photovoltage of two Ni-Cr contacts. At high energies a large negative photovoltage is observed which originates from the top Ni-Cr contact. The sign for the upper contact photovoltage is negative because the internal field pointing into the semiconductor points in a direction opposite to that at the lower contact.

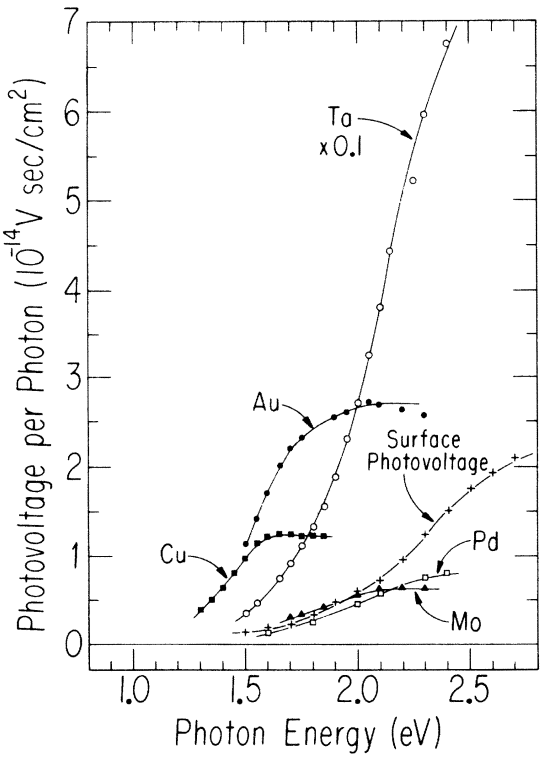

FIG. 5. Spectral response of photovoltage per photon absorbed in the semiconductor with different contacting metals. The magnitude of the contact photovoltage is observed to depend on the metal used. This indicates that the contact potential is not determined by surface states.

The peak at lower photon energies is the resultant of the two opposing photovoltages of the upper and the lower contacts. The fact that the positive sign of the lower contact photovoltage predominates despite the fact that more photons are absorbed at the upper contact, suggests that the internal field at the bottom Ni-Cr contact is larger than that at the top contact. Such asymmetry is possible even though the same contacting metal is used because the upper and lower contacts were prepared in different ways. At the lower contact the amorphous semiconductor was sputtered onto the Ni-Cr layer which was previously exposed to air. The top contact was prepared by evaporating Ni-Cr onto the amorphous layer.

We observe that (i) the photovoltage changes sign with wavelength of the incident light and (ii) a considerable photovoltage is obtained even at a wavelength at which the sample is nearly uniformly illuminated. This we take as evidence that one is dealing here with a barrier photovoltage near the contacts rather than with a Dember photovoltage cause by different diffusion rates of electrons and holes.[15]

Internal photoemission[16] of photoexcited electrons or holes from the metal into the semiconductor may also produce a photovoltage. It is difficult to distinguish the internal photoemission from the contact photovoltage in low-energy gap materials.[16] However, we believe that the contribution of the internal photoemission to the measured photovoltage in Fig. 4 is negligible because (i) the onset of the measured photovoltage is at 1.1 eV; this value is mich higher than 0.57 eV, the threshold for internal photoemission of carriers from the Fermi level of the metal to one of the bands in the semiconductor; (ii) the surface photovoltage is of the same order of magnitude as the contact photovoltage as shown in Fig. 5. The internal photoemission of electrons or holes is prohibited in this situation, since the metal probe electrode is separated from the free surface of the semiconductor. This will be discussed in Sec. III B.

Although internal photoemission is not prevented from occurring in our measurements of the contact photovoltage, we believe that it yields only a negligibly small photocurrent in these chalcogenide alloy glasses of low band gap because of the short lifetime of the excess carriers. For the same reason attempts to measure the drift mobility of excess carriers in these materials have failed.

The detailed shape of the photovoltage as a function of photon energy depends in a complicated way on the intensity spectrum of the incident light. This is because the photovoltage is proportional to the photon flux only at small light intensities. At high intensities the photovoltage increases as

the square root of the photon flux.[6] Furthermore, only photons absorbed in the space-charge region are probably contributing to the photovoltage and the internal field decreases from a maximum at the surface to zero through the width of the space-charge region. The photovoltage per absorbed photon in the semiconductor at 25 °C as a function of photon energy is shown for several metal contacts in Fig. 6. Considerably larger photovoltages were obtained for Ta and Ni-Cr contacts than for Pd, Sb, and Mo contacts. We observed that Au, Cu, Al, Pd, Pt, Ta, Mo and Ni-Cr yield a negative space charge; Sb contacts yield slightly positive, negative, or neutral contacts depending on the evaporation conditions. Te produces neutral contacts. The reason for this may be that Te is one of the major constituents of the sample and has similar electronegativity. The photovoltage varies with different contacting metals in a very complicated way. The larger photovoltages are generally observed for larger electronegativity differences between the metal and the semiconductor. However, no simple relationship has been obtained.

B. Surface photovoltage

The spectral response of the contact photovoltage shown in Fig. 4 can in principle be used to obtain an independent estimate of x_0, the width of the space-charge layer. However, since the contact photovoltage contains contributions from both contacts and possibly is altered by some alloying process as explained later, we decided to use the surface photovoltage instead.

The surface photovoltage technique for investigating the surface photoelectric properties of semiconductors has been widely used in the past.[17] When there is a difference of potential between the surface and the interior of a semiconductor, free carriers generated by photon absorption move under the influence of the electric field at the surface. The resulting displacement of charge may be detected by a capacitive probe near the surface and the corresponding potential difference is the so-called surface photovoltage.

The surface photovoltage of the same material was measured at a chopping frequency of 150 Hz at 24 °C. A thicker layer (about 6 μm) was used to avoid an additional photovoltage generated at the lower contact. The spectral response is shown in Fig. 6(a) for various light levels T.

The sign of the photovoltage indicates a negative space-charge region adjacent to the surface. If we assume that only those photons contribute to the surface photovoltage which create electron-hole pairs in the space region of width x_0, then the photovoltage can be written

$$V_{sp} = B\eta N_0 T(1-R), \tag{1}$$

$$\eta = 1 - \exp[-\alpha(h\nu)x_0], \tag{2}$$

where $N_0(h\nu)$ is the flux of incident photons, B is a constant, T is the transmittance of the Au film probe, and R is the reflectance of the sample. In this model the photovoltage is proportional to the spectral distribution of the incident light and the quantum efficiency η $(h\nu)$ of the photons in contributing to the photovoltage. We assume that the quantum efficiency is equal to the fraction of photons absorbed in the space-charge region of width x_0. This factor increases with increasing photon energies because of the increase of the absorption coefficient α. One expects η to saturate when the absorption coefficient is sufficiently large so that all photons are absorbed in the region x_0. Since we know from independent measurements N_0 and α as a function of photon energy, we can calculate the expected photovoltage for various space charge thicknesses x_0 and find the value which best fits the experimental results. Such a family of curves is shown in Fig. 6(b) by the dashed curves. The peak values have been normalized to unity. The

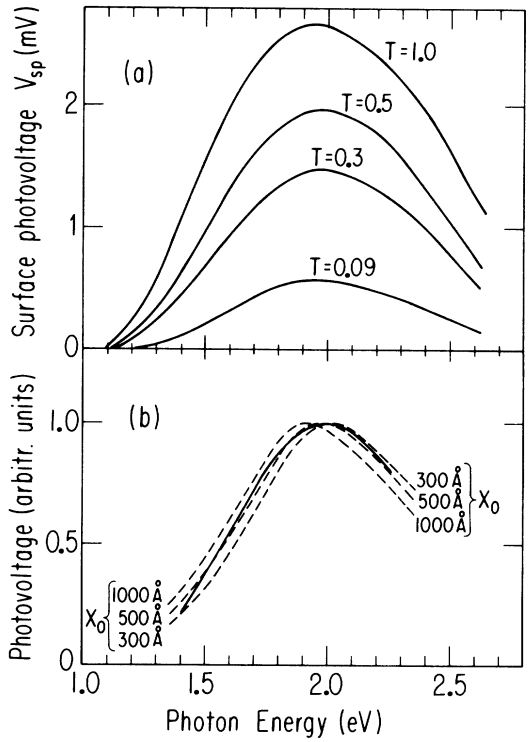

FIG. 6. (a) Spectral response of the surface photovoltage for various light intensities T. (b) Comparison of the measured photovoltage at low light intensity (full curve) with curves calculated from Eqs. (1) and (2) of text for various values of the space charge width x_0 (dashed curves).

heavy lines in Fig. 6 represent the measured spectral response of the surface photovoltage at low intensity where V_{sp} is linear with light intensity. A good fit to the experimental curves is obtained with x_0 between 300 and 500 Å for the surface photovoltage. This estimate of x_0 is not too accurate when x_0 is small because the absorption depth α^{-1} of the photons remains always larger than the width of the space-charge region. Moreover, this simple model does not take account of the fact that the internal field decreases rapidly to zero rather than being constant for $x < x_0$. Nevertheless, the comparison of the spectral response of the surface photovoltage shown in Fig. 6(b) suggests that the effective layer responsible for the surface photovoltage is of the order of a few hundred angstroms.

The effect of ambient gases on the surface photovoltage was studied.[18] The sample was kept in a steady flow of dry nitrogen gas for two days before the experiment. We found that the magnitude of the surface photovoltage increases as the relative humidity of water vapor in the nitrogen gas increased. The incremental increase of the surface photovoltage ΔV_{sp} divided by the original surface photovoltage V_{sp} in dry nitrogen as a function of the relative humidity of water vapor is shown in Fig. 7. We found that $\Delta V_{sp}/V_{sp}$ increases first linearly and then begins to saturate as the humidity increases. The surface photovoltage returns to the original value when the gas flow is changed to dry nitrogen. We found that the amount of the incremental increase and the leveling off point of the humidity depend on the surface conditions of the semiconductor. Similar phenomena of increasing V_{sp} with gas content were obtained with other polar molecule gases like NH_3, CO, CH_3COOH. Nonpolar gases like N_2, He, and O_2 yielded no effect. Reactive gases such as Cl_2 and O_3 cause irreversible decrease of the surface photovoltage as expected. We believe that the ambient effect on the surface photovoltage is caused by the absorption of polar molecules on the semiconductor surface. Charges transfer between polar molecules and surface states, thus inducing the change of the surface potential and the surface photovoltage.

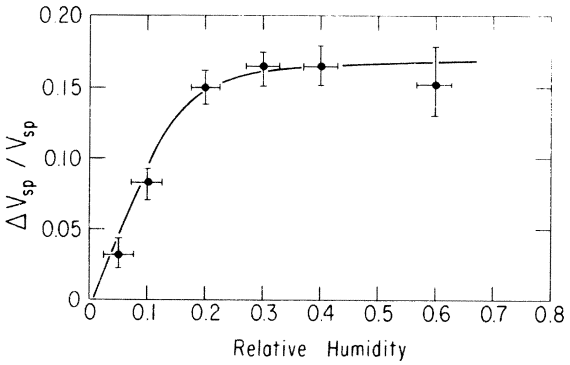

FIG. 7. Relative increase of surface photovoltage as a function of relative humidity in nitrogen at $T = 300$ K, photon energy $h\nu = 2.1$ eV, and chopping frequency = 80 Hz.

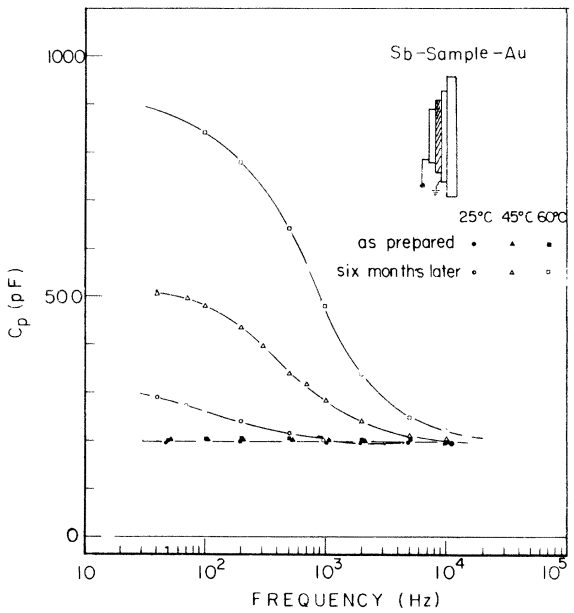

FIG. 8. Aging effect on Au contact. Parallel capacitance C_p rises at low frequencies after six months storage. This indicates that alloying took place at the Au contact.

C. Capacitance and alloy region

An estimate of the width of the space-charge region x_0 could be obtained from the spectral response of the surface photovoltage measurement in the previous section. We attempted to confirm this value for x_0 by measuring the equivalent parallel capacitance $C_p(\omega)$ as a function of frequency as that method is widely used in crystalline semiconductors.[5] We found however that $C_p(\omega)$ is independent of frequencies for all freshly prepared samples. This is not unexpected for the following reasons. Since the Fermi level lies near the gap center, any band bending near the surface tends to make the space-charge layer more conducting than the bulk. Under such conditions the dielectric relaxation time of the contact region is shorter than that of the bulk and the space-charge capacitance cannot be determined from $C_p(\omega)$ measurement because the C_p will be independent of frequency. In some cases, on the other hand, we did observe a strong increase of $C_p(\omega)$ at low frequencies as shown in Fig. 8. This behavior signifies the presence of a high-resistance layer ad-

jacent to the contact. As discussed below, this layer is caused by alloying and does not represent a depletion layer.

1. Aging effect and annealing effect on Au *contacts*

Capacitance measurement on a sample with Sb-sample-Au structure showed that C_p and R_p were independent of measuring frequencies when it was freshly prepared. After six months, however, $C_p(\omega)$ was found to rise at low frequencies as shown in Fig. 8. Furthermore, the I-V curves deviated noticeably from the original ohmic behavior. The photovoltage measurement, on the other hand, showed no noticeable change after six months.

On the same substrate, another sample prepared as a Sb-sample-Sb structure, showed no change in the $C_p(\omega)$, I-V, and the photovoltage measurement. It is very clear that something happened at the semiconductor-Au interface. We believe it is slow alloying of Au with the amorphous semiconductor.

We found that the slow alloying process of Au

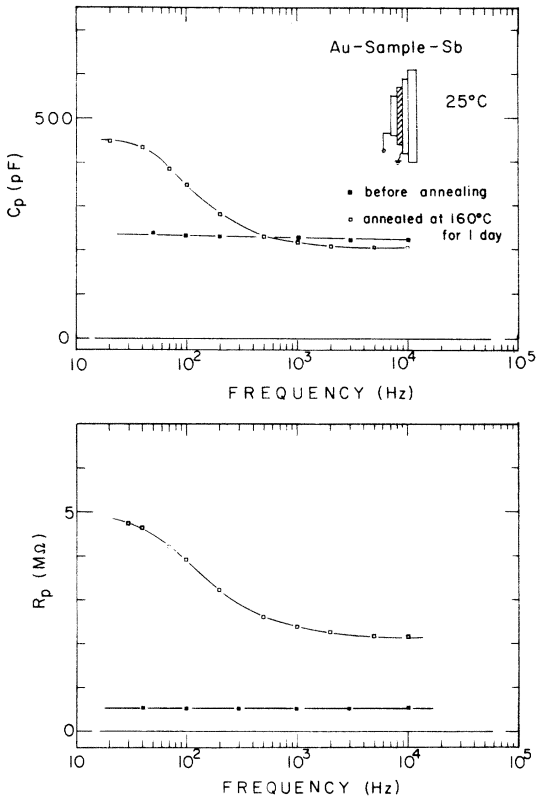

FIG. 9. Annealing effect of Au contact. Parallel capacitance C_p and parallel resistance R_p rise at low frequencies after annealing the sample at 160 °C for 24 h. This change of contact behavior with annealing indicates that the alloying process is accelerated by elevating the temperature.

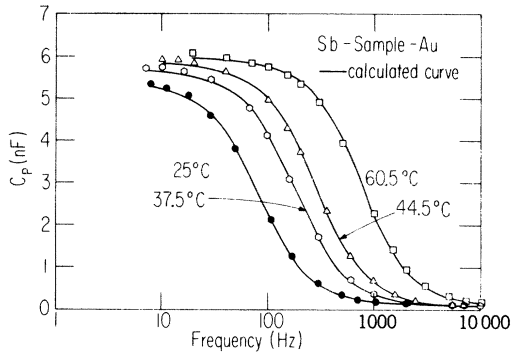

FIG. 10. Frequency dependence of parallel capacitance of sample with Sb and Au contacts measured at four different temperatures. Solid lines calculated from Eq. (3) of text show that the experimental data can be fitted by the parameters listed in Table I.

with the amorphous semiconductor can be accelerated by annealing the sample at higher temperature. The capacitance was independent of frequency before annealing as shown in Fig. 9. After annealing the sample at 160 °C for 24 h, the capacitance rises at low frequencies. No rise of C_p at low frequencies was observed for the sample with Sb-sample-Sb structure. We therefore conclude that the alloying process on the Au contact was enhanced by the annealing.

2. Analysis of the C_p (ω) *measurements*

The frequency dependence of the parallel capacitance and resistance measured at various temperatures on a sandwich sample with Sb and Au as electrodes as that of Fig. 8, are shown in Figs. 10 and 11, respectively. The capacitance at low

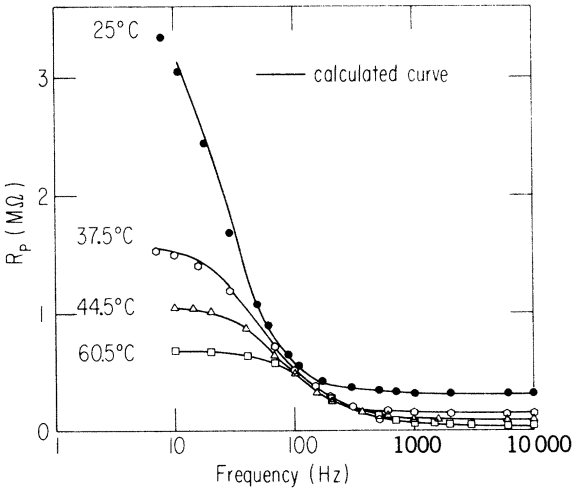

FIG. 11. Frequency dependence of parallel equivalent resistance of sample used for Fig. 11. Theoretical curves use the same parameters listed in Table I.

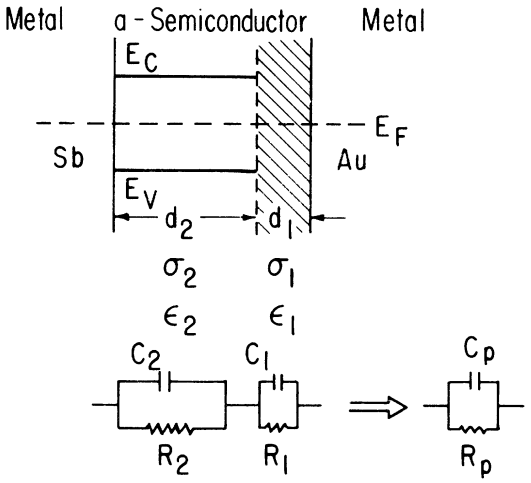

FIG. 12. Equivalent circuit used for analysis.

frequencies is about 40 times higher than that at high frequencies. This behavior is analyzed by assuming the equivalent circuit shown in Fig. 12, where the alloy region of thickness d_1 is represented by the capacitance C_1 and resistance R_1 and the bulk region of thickness d_2 by a capacitance C_2 and resistance R_2.

The equivalent parallel C_p and resistance R_p are

$$C_p = \frac{R_1^2 C_1 + R_2^2 C_2 + \omega^2 R_1^2 R_2^2 C_1 C_2 (C_1 + C_2)}{(R_1 + R_2)^2 + \omega^2 R_1^2 R_2^2 (C_1 + C_2)^2} \tag{3}$$

and

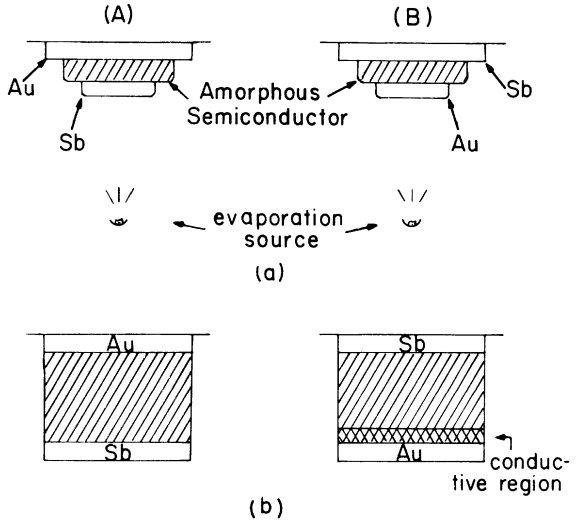

FIG. 13. (a) Two samples prepared simultaneously but with opposite structures. Amorphous semiconductor was sputtered onto the Au electrode in sample A, while the Au electrode was evaporated onto the amorphous semiconductor. (b) High-conductivity region near the Au electrode was found in sample B.

TABLE I. Best values for C_1, R_1, C_2, and R_2.

Temperature (°C)	C_1 (pF)	R_1 (kΩ)	C_2 (pF)	R_2 (kΩ)
25	6200	3480	153	317
37.5	6650	1460	153	141
44.5	6800	960	153	88.8
60.5	6500	650	153	33.3

$$R_p = \frac{(R_1 + R_2)^2 + \omega^2 R_1^2 R_2^2 (C_1 + C_2)^2}{(R_1 + R_2) + \omega^2 [R_2 (R_1 C_1)^2 + R_1 (R_2 C_2)^2]} . \tag{4}$$

If we assume that $C_1 \gg C_2$ we obtain the following asymptotic values for low frequencies ($\omega \to 0$) and high frequencies ($\omega \to \infty$), respectively,

$$C_p(0) \approx C_1 R_1^2 / (R_1 + R_2)^2$$

and

$$C_p(\infty) = C_1 C_2 / (C_1 + C_2) \approx C_2 \tag{5}$$

$$R_p(0) \approx R_1 + R_2 \quad \text{and} \quad R_p(\infty) \approx R_2 .$$

The geometric capacitance $C_2 \approx C_p(\infty)$ and the total resistance $R_p(0) = R_1 + R_2$ can be measured with good accuracy. The remaining quantities C_1 and the ratio $F = R_2/R_1$ were determined by least-square fitting Eq. (3) to the experimental points of Fig. 9. The quantities thus determined are listed in Table I for various temperatures. The full curves in Figs. 10 and 11 represent calculated curves using Eqs. (3) and (4) with these values.

With the measurements of film thickness $d = 1.77 \pm 0.2$ μm, and the contact area $A = 2.4 \times 10^{-2}$ cm^2 we obtain at 25 °C a bulk resistivity $\rho_2 = 4 \times 10^7$ Ω cm, and an effective resistivity of the alloy region $\rho_1 = 2 \times 10^{10}$ Ω cm, a dielectric constant $\kappa = 12.7$, and for the width of alloy region $d_1 = 420 \pm 50$ Å. The thermal activation energy obtained from the temperature dependence of the bulk resistance R_2 was found to be $E = 0.57$ eV in agreement with previous measurements on this material. The thickness of the alloy region depends on the contacting metals, the preparation conditions, aging and annealing, but it is usually about 100–500 Å.

The alloying process between the metal and the semiconductor depends on the preparation method and conditions. We found a high-conductivity region near the Au contact instead of a high-resistivity region when the preparation method was changed in the following manner. Two samples were prepared simultaneously but with opposite structure as shown in Fig. 13. The amorphous semiconductor was sputtered onto the Au electrode in sample A, whereas the Au electrode was evaporated onto the semiconductor in sample B. We found for the resistances $R_A > R_B$, and the capacitances $C_A < C_B$. Of interest is that the prod-

uct of R and C is constant, that is $R_A C_A \approx R_B C_B$. Since the areas of the two samples were the same, it appears that the thickness of sample B was (10–15)% less than that of sample A. The same was observed with nichrome contacts. This reduction of the effective thickness of the semiconductor becomes larger when the evaporation source is closer to the substrate. It appears that a high-conductivity region is produced as a result of diffusion of impinging metal atoms, when a high melting point metal is evaporated onto an amorphous semiconductor.

IV. DISCUSSION AND SUMMARY

One expects a space-charge region to exist in amorphous semiconductors adjacent to contacts or to the surface for the same reason as those which cause such regions in crystalline semiconductors. When a metal is placed in contact with an amorphous semiconductor, the different work function of the metal and the semiconductor causes charge transfer from one material into the other until their Fermi levels are equalized. A space-charge layer of the appropriate sign will then occur inside the semiconductor. If there is a considerable density of surface states[19] or interface states on the semiconductor surface, a space-charge region will also occur. However, in this case charges transfer between contacting metals and the surface states, and the space-charge region is less affected by the metal work function. Three important parameters characterize the space-charge region: the barrier height or surface potential V_s, the width of the space-charge region x_0, and the density of surface states.

Space charge width x_0 obtained in Sec. III B yields the density of gap states at the Fermi level E_F. We assume a constant density of localized gap states near E_F. In that case the band bending potential $U(x)$ produces a charge density $\rho(x) = -e^2 g(E_F) U(x)$, and the solution of Poisson's equation

$$\frac{d^2U(x)}{dx^2} = \frac{U(x)e^2 g(E_F)}{\kappa \epsilon_0} \tag{6}$$

yields the potential

$$U(x) = U(0) \exp(-x/x_0) , \tag{7}$$

with the characteristic screening length

$$x_0^2 = \kappa \epsilon_0 / e^2 g(E_F), \tag{8}$$

where κ is the dielectric constant and $\epsilon_0 = 8.86 \times 10^{-14}$ F/cm. The charge per unit area Q, is related to the field at the interface $U(0)/x_0$ as

$$Q = \kappa \epsilon_0 U(0)/x_0 . \tag{9}$$

For the particular potential distribution of Eq. (7) one finds that the effective space-charge width defined as

$$\int_0^\infty x \rho(x)\, dx \Big/ \int_0^\infty \rho(x)\, dx \tag{10}$$

is equal to the screening length x_0.

An appreciable number of localized gap states is required to account for the short screening length $300 < x_0 < 500$ Å observed. Assuming for simplicity a constant density of states model which leads to Eq. (8) we obtain $2 \times 10^{17} < g(E_F) < 8 \times 10^{17}$ eV^{-1} cm^{-3} with $\kappa = 12.7$.

The values of $g(E_F)$ deduced from the surface photovoltage measurements are much too low to account for the small magnitude of the field effect observed by Egerton[19] and Arnoldussen *et al.*[19] in a number of chalcogenide alloy glasses. We therefore conclude that an appreciable density of localized states must be present at the surface or interface with the insulator used in the field effect studies. The interface state density must be about 10^{14} cm^{-2} eV^{-1} near the Fermi level. Such interface state densities are not uncommon in crystalline semiconductors.

In crystalline semiconductors, three methods,[5] I-V, $C(V)$, and internal photoemission, are commonly used to measure the barrier heights of metal-semiconductor contact. However, difficulties arise when these methods are applied to measure the barrier heights of metal-amorphous semiconductor contacts. One usually finds a low-contact resistance and small rectification ratios in amorphous semiconductors. We believe the principal reason for this is the following.[10] The Fermi level in most amorphous semiconductors is close to the gap center. In this case, the reverse bias saturation current is much larger and the bulk conductivity much smaller compared to the case when E_F is close to one of the band edges as in a crystalline semiconductor. Thus conduction can take place in one band in the space-charge region and in the other band in the bulk with the generation and recombination processes equilibrating the two currents at the onset of the space-charge region. In other words, the near intrinsic character of amorphous semiconductors assures a low contact resistance relative to the bulk resistance and a small rectification ratio.[5,10] The applied voltage drop occurs mainly in the bulk region instead of the contact region. Thus, the information about the barrier height V_s and the width of space-charge region x_0 can not easily be extracted from the I-V and $C(V)$ measurements.

The internal photoemission method can only be useful when the barrier height is $\gtrsim 40\ kT$. As discussed by Williams,[16] when small barrier heights are involved it can be very difficult to distinguish between photoemission and enhanced

thermionic emission from the metal due to the small temperature rise from the absorption of light by the metal. No other measurements of the barrier heights of low-energy gap amorphous semiconductors with metal contact are known so far.

Mead *et al.*[20] studied the barrier height of a large class of crystalline semiconductors and insulators with different contacting metals. They found the measured barrier energy ϕ_B of various metals on a semiconductor was in general proportional to the electronegativity X_M of the metals, or

$$\phi_B \approx S X_M + \text{const.} \tag{11}$$

This proportionality constant S was called the index of interface behavior. They found two groups of semiconductors with distinctively different barrier behaviors. For high band gap, in ionically bonded semiconductors such as SiO_2 and Al_2O_3 the barrier heights usually vary proportionally with the work functions or electronegativities of the contacting metals, i.e., their index of interface behavior $S \sim 1.0$. For low band gap (covalently bonded semiconductors such as Ge and Si) the barrier heights are nearly independent of the work functions or electronegativities of the contact metals, i.e., their index of interface behavior $S \sim 0$. Semiconductors like GaSe and CdS lie in the transition region with $S \sim 0.6$. Our sample material with electronegativity difference $\Delta X \sim 0.7$ is located near $S \sim 0.2$ on Mead's plot. This suggests that the barrier heights vary slightly with the work function of the contacting metals.[21] This agrees with our results shown in Fig. 5 and with the observation that the surface potential is changed by the absorption of gases.

The increase of the parallel capacitance $C_p(\omega)$ at low frequencies requires a high-resistivity region adjacent to the contact. The aging effect and annealing effect shown in Figs. 8 and 9 indicate that this high-resistivity region originates from the alloying of the metal electrode with the amorphous semiconductor instead of the space charge region as postulated by Wey and Fritzsche.[6,22] Depending on the chemical properties of the contacting metals, different alloy regions may occur. Contact effects for several metals with $Ge_{16}As_{35}Te_{28}S_{21}$ have been studied. We found that Ag and Cu react strongly with the sample. One can even measure a small dc voltage across the electrodes, which indicates that a chemical reaction is taking place. Several hundred angstroms thick Ag or Cu electrodes will react completely with the sample in a few days. Au and nichrome alloy slowly with the sample. Similar results have been found by Nielsen[23] with amorphous Se and Cu, Ag, Al. The formation of a selenide layer at the interface between Cu, Ag, and Al electrodes and amorphous Se was observed in the change of the energy distribution curves of photoemitted electrons from the surface of Cu, Ag, or Al, when he deposited successive layers of amorphous Se films. Electron microscope studies by Freeman *et al.*[24] showed that Au diffuses and alloys slowly with As_2Se_3. Backscattering data of Mayer[25] on a silicon-metal system also suggested the formation of metal-silicide and the migration of metals at the interface with crystalline silicon. Ge and Te are constituent elements of the sample. No alloying regions were expected or found. Al, Ta, and Ti oxidize easily. An insulating oxide layer formed at the interface tends to give high contact resistances. No alloying, contact resistance and only a very small photovoltage were found with Sb, Pt, Pd, and Mo.

A high conductivity region occurs at the Au or nichrome interface with the amorphous semiconductors described in Sec. III C, when these high melting point metals are evaporated onto the semiconductors. Similar results have also been found by Strunk[26] with the As_xSe_{1-x} system. The nature of this high-conductivity region remains to be studied. Methods like backscattering technique,[27] or ion-probe analysis may be able to provide more information about the nature of this high-conductivity region.

ACKNOWLEDGMENTS

The author wishes to thank M. Kastner, S. Chandra, S. Hudgens, M. Paesler, C. Tsai, and I. Shimizu for many valuable discussions; his parents and K. Kang for continuing encouragement; J. Yang and P. Gaczi for technical assistance. Most of all, the guidance, encouragement, and support of his thesis advisor, Professor H. Fritzsche, are greatly appreciated.

---

*Research supported by the Air Force Office of Scientific Research (AFSC), U. S. Air Force under Contract No. F44620-71-C-0025, and aided through general support of the Materials Research Laboratory by the NSF at the University of Chicago.

†Submitted in partial fulfillment of the requirements for the Ph.D. degree at The University of Chicago.

‡Present address: Westinghouse Research and Development Center, Pittsburgh, PA. 15235.

[1]S. R. Ovshinsky, Phys. Rev. Lett. 21, 1450 (1968).

[2]Morrel H. Cohen, H. Fritzsche, and S. R. Ovshinsky, Phys. Rev. Lett. 22, 1065 (1969).

[3](a) N. F. Mott and E. A. Davis, *Electronic Processes in Non-Crystalline Materials* (Clarendon, Oxford, 1971); in (b) *Amorphous and Liquid Semiconductors*, edited by J. Tauc, (Plenum, New York, 1974).

[4]H. K. Henisch, *Rectifying Semiconductor Contacts* (Clarendon, Oxford, 1957); A. Many, Y. Goldstein, and N. B. Grover, *Semiconductor Surfaces* (North-Holland, Amsterdam, 1965).

[5]S. M. Sze, *Physics of Semiconductor Devices* (Wiley, New York, 1969).

[6]H. Y. Wey and H. Fritzsche, J. Non-Cryst. Solids 8–10, 336 (1972); H. Y. Wey, Bull. Am. Phys. Soc. 17, 345 (1972).

[7]R. Grigorovici, N. Croitoru, A. Devenyi, and E. Teleman, in *Proceedings on the Seventh International Conference on the Physics of Semiconductors*, edited by M. Hulin (Academic, New York, 1954), Vol. VII, p. 423; L. A. Zhurakovskii, A. Kh. Zeinally, B. T. Kolomiets, and N. A. Krasilnikiva, Fiz. Tekh. Poluprovodn. 5, 1917 (1971) [Sov. Phys.-Semicond. 5, 1665 (1972)]; D. Alder, *Anorphous Semiconductors* (CRC Press, Cleveland, 1971).

[8]P. J. Walsh, R. Vogel, and E. J. Evans, Phys. Rev. 178, 1274 (1969); E. A. Fagen and H. Fritzsche, J. Non-Cryst. Solids 2, 170 (1970); A. E. Owen and J. M. Robertson, IEEE Trans. Electron Devices ED-20, 105 (1973).

[9]H. Fritzsche, in Ref. 3(b), Chap. 6.

[10]H. Fritzsche, in Ref. 3(b), Chap. 5.

[11]Purchased from Energy Conversion Devices, Inc., Troy, Michigan.

[12]H. Y. Wey (unpublished).

[13]E. A. Fagen, R. S. Nowicki, and R. W. Seguin, J. Appl. Phys. 45, 50 (1974).

[14]P. Gaczi, H. Y. Wey, and H. Fritzsche (unpublished).

[15]S. R. Ryvkin, *Photoelectric Effects in Semiconductors* (Consultants Bureau, New York, 1964).

[16]J. Mort and A. J. Lakatos, J. Non-Cryst. Solids 4, 117 (1970); R. Williams, in *Semiconductors and Semi-Metals*, edited by R. K. Willardson and A. C. Beer (Academic, New York 1970), Vol. 6, Chap. 2; J. S. Helman and F. Sanchez-Sinencio, Phys. Rev. B 7, 3702 (1973).

[17]W. H. Brattain and C. G. B. Garrett, Bell Syst. Tech. J. 35, 1019 (1956); E. O. Johnson, RCA Rev. 18, 556 (1957); D. R. Frankl and E. A. Ulmer, Surf. Sci. 6, 115 (1966).

[18]H. Y. Wey and H. Fritzsche, in *Proceedings of the Eleventh International Conference on the Physics of Semiconductors*, 1972 (Polish Scientific Publ., Warsaw, 1972), p. 555.

[19]G. W. Neudeck and A. K. Malhotra, J. Appl. Phys. 46, 239 (1975); T. C. Arnoldussen, C. A. Menezes, Y. Nakagawa, and R. H. Bube, Phys. Rev. B 9, 3377 (1974); R. F. Egerton, Solid State Commun. 10, 1081 (1972).

[20]S. Kurtin, T. C. McGill, and C. A. Mead, Phys. Rev. Lett. 22, 1433 (1969); T. C. McGill, J. Vac. Sci. Technol. 11, 935 (1974); J. C. Phillips, *ibid.* 11, 947 (1974).

[21]J. Mort and A. J. Lakatos, J. Non-Cryst. Solids 4, 117 (1970); P. Nielsen, Solid State Commun. 9, 1745 (1971).

[22]H. Fritzsche, in *Electronic and Structural Properties of Amorphous Semiconductors*, edited by P. G. Le Comber and J. Mort (Academic, London, 1973).

[23]P. Nielsen, Thin Solid Films 15, 309 (1973).

[24]L. A. Freeman, R. F. Shaw, and A. D. Yoffe, Thin Solid Films 3, 367 (1969).

[25]J. W. Mayer, Bull. Am. Phys. Soc. 20, 280 (1975).

[26]R. Strunk, Ph.D. thesis (Rheinisch-Westfalischen Technischen Hochschule Aachen, 1973) (unpublished), p. 90.

[27]G. Ottaviani, D. Sigurd, V. Marrello, J. W. Mayer, and J. O. McCaldin, J. Appl. Phys. 45, 1730 (1974).